Exciton dephasing in self-assembled CdSe quantum dots

Phedon Palinginis and Hailin Wang
Department of Physics, University of Oregon, Eugene, Oregon 97403, USA

Serguei V. Goupalov
Theoretical Division, Los Alamos National Laboratory, Los Alamos, New Mexico 87545, USA
and A.F. Ioffe Physico-Technical Institute, 194021 St. Petersburg, Russia

D. S. Citrin
School of Electrical and Computer Engineering, Georgia Institute of Technology, Atlanta, Georgia 30332-0250, USA

M. Dobrowolska and J. K. Furdyna
Department of Physics, University of Notre Dame, Notre Dame, Indiana 46556, USA
(Received 30 March 2004; published 9 August 2004)

We report experimental studies of exciton dephasing in self-assembled CdSe quantum dots using techniques based on spectral hole burning. The hole-burning response reveals directly in the spectral domain the zero-phonon-line (ZPL) as well as contributions from acoustic and LO-phonon assisted transitions. The observed strong coupling to acoustic phonons is in good agreement with theoretical expectation. The measured decoherence rate associated with the ZPL is as small as 3.5 μeV, comparable to that in self-assembled InGaAs quantum dots.

DOI: 10.1103/PhysRevB.70.073302 PACS number(s): 73.21.La, 78.67.Hc

Recent observations of Rabi oscillations[1] and photon antibunching[2] in single quantum dots (QDs) have demonstrated their remarkable atom-like characteristics. Despite these striking similarities, semiconductor QDs are fundamentally different from atomic systems as electrons in a QD can couple to the vibrational modes of the crystal lattice. Consequently, electron–phonon interactions play a dominant role in the decoherence of optical excitations in QDs. Experimental studies of decoherence and electron–phonon interactions in QDs have employed a variety of techniques, including photoluminescence (PL) of single QDs and nonlinear optical spectroscopy. Most PL studies of single self-assembled III–V and II–VI QDs have shown sharp zero-phonon lines (ZPL) with linewidths on the order of 50–100 μeV, limited by spectral resolution and/or by effects of spectral diffusion induced by fluctuations in the local environment[3,4]. In contrast, recent transient four-wave mixing studies in self-assembled InGaAs QDs have shown an intrinsic ZPL linewidth as small as a few μeV[5]. Theoretical studies of dipole decoherence in QDs have been carried out within the independent boson model.[6–9] While including phonon-assisted transitions as the main source for pure dephasing[10], this model does not account for broadening of the ZPL due to electron–phonon interactions. More recent studies have attempted to account for broadening of the ZPL in extensions of the independent boson model.[11,12]

In this paper we report experimental studies of exciton dephasing and effects of spectral diffusion in self-assembled CdSe QDs using high resolution spectral hole burning (SHB). Theoretical calculations of the linear absorption spectrum of CdSe QDs are also presented. The SHB response reveals directly in the spectral domain the ZPL as well as the characteristic features associated with acoustic–phonon and LO-phonon assisted transitions. The contribution from acoustic–phonon assisted transitions is in general agreement with theoretical expectation. The ZPL linewidth obtained from the SHB response depends sensitively on the measurement timescale, indicating the presence of spectral diffusion. Being able to suppress the effects of spectral diffusion in SHB, we have obtained ZPL linewidths as small as a few μeV, comparable to that in InGaAs QDs. The temperature dependence of the ZPL linewidth further suggests that electron–phonon interactions contribute to decoherence of the ZPL via spin relaxation and thermal activation of excitons to higher lying states.

The CdSe QDs used in this work were grown on top of a ZnSe buffer by molecular beam epitaxy.[13] Reflection high-energy electron diffraction (RHEED) was used to monitor the CdSe deposition. At a film thickness of 2.5–3 ML monolayers the RHEED pattern showed a clear transition from streaky to spotty, indicating the onset of island formation. The resulting CdSe QDs were capped with a ZnSe layer to prevent island ripening. For transmission measurements, the sample was mounted on a sapphire disk and the GaAs substrate was removed with selective chemical etching. Low-temperature measurements ($T > 4.2$ K) were carried out using a cold-finger cryostat. For measurements down to 1.8 K, a helium-flow cryostat was used. Two frequency-stabilized tunable ring dye lasers (CR 699 and CR 899, Coherent, Inc.) were used to provide pump and probe beams in the SHB measurement. The spectral resolution is limited by the relative laser jitter and is less than 3 MHz ($\sim$10 μeV). The change in the probe transmission induced by the pump was measured using lock-in detection, with the pump intensity modulated by an acousto-optic modulator (AOM).

Figure 1 shows the SHB response (normalized differential transmission $\Delta T/T$) at 10 K as a function of the pump–probe detuning. The pump energy is set at $E_{\text{pump}} = 2.16$ eV as indi-

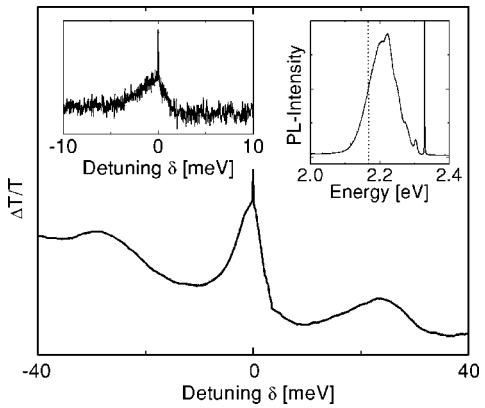

FIG. 1. SHB spectrum at $T=10$ K($\Omega=10$ kHz, $I_{\text{pump}}=2I_{\text{probe}}=2$ W/cm^2). The inset on the right shows the PL spectrum for excitation in the wetting layer; the dotted line indicates the pump energy used in the SHB. The inset on the left shows an expanded scan of the ZPL and acoustic phonon pedestal $\Omega=3$ MHz.

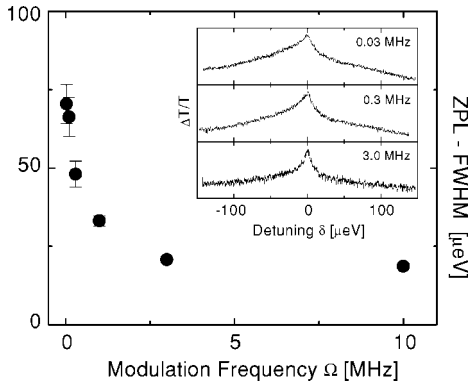

FIG. 2. Modulation frequency dependence of the ZPL linewidth at $T=10$ K($I_{\text{pump}}=10I_{\text{probe}}=4$ W/cm^2). The inset shows high-resolution scans of the ZPL demonstrating a narrowing of the ZPL.

cated by the dashed line in the PL spectrum shown in the inset of Fig. 1 (the PL spectrum shows a characteristic LO-phonon progression as expected for excitation with $E_{\text{exc}}=2.33$ eV in the wetting layer, indicative of efficient capture of the photoexcited carriers in the CdSe islands). Similar SHB spectra have been obtained with the pump energy fixed at various spectral positions in the lower part of the PL spectrum. Carrying out the SHB in the low energy part of the PL spectrum ensures that contributions from higher excited states to the SHB response are minimized. Disregarding the overall slope of the SHB response, which results from difficulties associated with normalization, i.e., measurements of the weak sample absorption ($\alpha L<0.5\%$), the SHB response shown in Fig. 1 reveals three features: a sharp resonance at zero detuning, a broad asymmetric pedestal centered around zero detuning, and two sidebands with similar broadening.

We infer from the sideband splitting ($\sim$26 meV) that the two sidebands arise from LO-phonon assisted optical transitions. The appearance of both Stokes and anti-Stokes sidebands may seem surprising, since at 10 K thermal population of LO phonons is negligible. For the sideband at positive detuning the pump is resonant with the zero phonon transition, while the probe is resonant with the transition assisted by the emission of a LO phonon. For the sideband at negative detuning the probe is resonant with the zero phonon transition, while the pump is resonant with the transition assisted by emission of a LO phonon. Thus, both LO-phonon sidebands observed in low-temperature SHB involve predominantly the emission of LO phonons in the optical process.

The sharp SHB resonance at zero detuning corresponds to the ZPL and arises when pump and probe couple to QDs for which the zero–phonon transition is resonant with the incident fields. In the $\chi^{(3)}$-limit and for systems with only static inhomogeneous broadening, the full width at half-maximum (FWHM) of the ZPL is twice the homogeneous linewidth of the purely electronic transition (FWHM$=4\gamma$, where γ is the intrinsic dephasing rate for the ZPL). This is no longer true, however, if the transition frequency is subject to fluctuations in the local environment. Then, in the presence of so-called spectral diffusion, the linewidth of the SHB resonance depends on the time scale of the measurement. The effects of spectral diffusion on the SHB response, however, can be greatly reduced if the measurement time scale is short compared with the time scales involved in spectral diffusion.[14] For lock-in detection of the SHB response, the measurement time scale is set by the modulation period of the pump intensity, which in our case can be as short as 100 ns. In contrast, integration times are on the order of seconds in typical PL measurements. It should be noted that excitation levels as low as a few W/cm^2 are used in the SHB measurement, which is two orders of magnitude smaller than in typical single-dot PL measurements.

Figure 2 shows the FWHM of the ZPL in the SHB response as a function of the modulation frequency Ω obtained at 10 K. The inset in Fig. 2 shows high-resolution spectra of the ZPL for $\Omega=0.03$, 0.3, and 3 MHz. The spectra clearly reveal a narrowing of the ZPL with increasing modulation frequency, indicating the presence of spectral diffusion in self-assembled CdSe QDs. The ZPL linewidth remains nearly unchanged for $\Omega>3$ MHz. The effects of spectral diffusion on the ZPL linewidth are thus suppressed at these high modulation frequencies and low excitation levels ($I_{\text{pump}}=4$ W/cm^2). The details of the microscopic origin of spectral diffusion in self-assembled QDs are still poorly understood, with carrier trapping or fluctuations in the strain field being possible mechanisms.

We have further examined the temperature dependence of the ZPL in a regime where spectral diffusion is suppressed. Figure 3(a) shows a sequence of high-resolution SHB spectra at various temperatures obtained at $\Omega=3$ MHz and $I_{\text{pump}}=4$ W/cm^2. Note that power broadening is negligible at this excitation level, as shown in the intensity dependence in the inset of Fig. 3(b). The temperature dependence of the dephasing rate γ obtained from the linewidth of the SHB response is shown in Fig. 3(b). Extrapolation of the experimental data yields a dephasing rate of $\gamma_0=3.5$ μeV at zero temperature, corresponding to a dephasing time of 200 ps.

Within the framework of the independent boson model and a linear coupling mechanism, electron–phonon interactions in a QD can lead to phonon-assisted transitions that involve absorption or emission of phonons, yet without re-

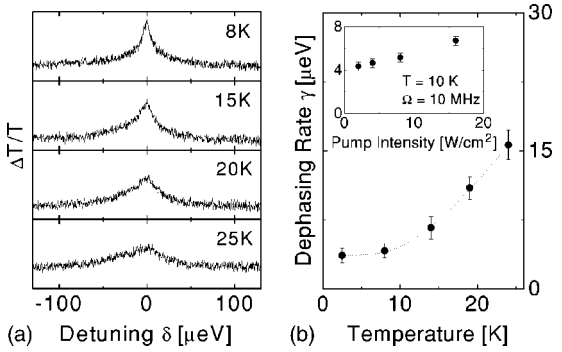

FIG. 3. (a) Temperature dependence of the ZPL ($\Omega = 3$ MHz and $I_{\text{pump}} = 10 I_{\text{probe}} = 4$ W/cm^2); (b) dephasing rate as obtained from (a). The dotted line is a guide to the eye. The inset shows the pump intensity dependence.

sulting in a spectral broadening of the ZPL[9]. In self-assembled CdSe QDs, electron-hole exchange interactions lead to a fine structure of dipole-allowed (bright) and dipole-forbidden (dark) states in the heavy-hole exciton manifold, with the dark states lying energetically below the bright state. An earlier magneto-optical study has shown a bright-dark exciton splitting ranging between 1.7 and 1.9 meV for self-assembled CdSe QDs.[15] Spin relaxation of the bright exciton to the dark states via emission of acoustic phonons could lead to decoherence of the ZPL, as suggested in an earlier theoretical study.[12] This process can provide a decoherence mechanism for the ZPL even at zero temperature. A numerical fit of the observed temperature dependence shows that acoustic–phonon emission alone cannot account for the experimental result. Thermal activation into higher lying states via absorption of acoustic phonons also provides additional decoherence channels. Given the limited temperature range over which the ZPL persists (the ZPL disappears near 30 K), we have not been able to extract reliably the relevant physical parameters, including bright-dark exciton splitting and the thermal activation energy, from the temperature dependence. Nevertheless, the strong temperature dependence of the ZPL linewidth indicates a significant contribution from electron-phonon interactions to decoherence of the ZPL.

We now turn to the broad pedestal in the SHB response. Similar to LO-phonon assisted transitions, pump and probe can couple to different transitions in the manifold of the zero–phonon and acoustic–phonon assisted transitions in SHB giving rise to acoustic–phonon sidebands. Integration over the continuum of acoustic–phonon sidebands results in the broad pedestal observed in the SHB response. The similar linewidths of the LO-phonon sidebands and the acoustic–phonon pedestal shown in Fig. 1 further indicate that acoustic-phonon assisted transitions also contribute to the mechanism giving rise to the LO-phonon sidebands.[9]

For a more detailed understanding of the acoustic-phonon assisted transitions, we have calculated the absorption spectrum of a single QD based on a model in which a two-level system is coupled to a continuum of acoustic–phonons via deformation potential coupling. While ZPL broadening is not included, the model is able to predict the relative spectral weight of the ZPL and the acoustic–phonon pedestal. The

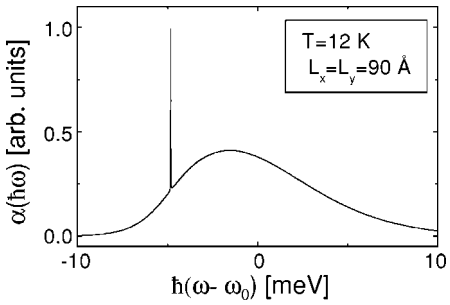

FIG. 4. Calculated linear absorption spectrum for a CdSe QD at 12 K($L_z = 1.1$ nm) with deformation potential coupling constants $D_e = 11$ eV and $D_h = 8.9$ eV (Ref. 16).

calculation follows essentially the steps outlined in Ref. 12. The absorption cross section is obtained from Kubo's formula,

$$\sigma(\omega) \propto \int_0^\infty dt[\mathrm{Re}[U(t)]\cos(\omega - \omega_0)t - \mathrm{Im}[U(t)]\sin(\omega - \omega_0)t], \tag{1.1}$$

where ω_0 is the transition frequency of the two-level system in the absence of electron–phonon interactions; $U(t)$ is given by $U(t) = e^{K(t)}$, where $K(t)$ has the form:

$$K(t) = -\gamma_{\mathrm{ZPL}} t + \frac{1}{V}\sum_q \frac{|A_q|^2}{\omega_q^2}\left[(\cos\,\omega_q t - 1)\coth\frac{\hbar\omega_q}{2T} - i(\sin\,\omega_q t - \omega_q t)\right], \tag{1.2}$$

ZPL broadening is added phenomenologically and γ_{ZPL} is taken from the experiment. The sum runs over all longitudinal acoustic modes with wave vectors $\boldsymbol{q}$, and frequencies $\boldsymbol{\omega_q}$; T denotes temperature, V is the normalization volume. Electron–phonon interactions enter via the Huang–Rhys factors $|A_{\boldsymbol{q}}|^2/\omega_{\boldsymbol{q}}^2$ and depend sensitively on the bulk electron/hole deformation coupling constant and the form factor, which is determined by the dot size and shape.

Figure 4 shows numerical results for the linear absorption spectrum of a single CdSe QD embedded in ZnSe. For ease of calculation, a square shape confining potential is taken for in-plane motion ($L_x = L_y = 9$ nm); confinement along the growth direction is determined by the square well potential of the wetting layer ($L_z = 1.1$ nm). A polaron shift (~ 5 meV) is revealed, as well as an acoustic–phonon pedestal whose asymmetric line shape indicates that optical transitions assisted by emission rather than absorption of phonons dominate at low temperature. Comparison of the spectral weight ratio η between the ZPL and the overall acoustic–phonon pedestal shows good agreement with the experiments. The numerical calculation also shows a rapid decrease of the relative ZPL contribution with increasing temperature, with the ZPL disappearing near 30 K (not shown), again in good agreement with the experiment. It should be added that, while $\eta \sim 0.01$ is obtained for CdSe self-assembled QDs ($T = 10$ K), additional calculations show $\eta \sim 1$ for InGaAs self-assembled QDs ($T = 10$ K), confirming

the much stronger electron–acoustic phonon coupling in CdSe QDs.

In summary, high resolution SHB studies allow us to suppress the effects of spectral diffusion, and thus to measure directly in the spectral domain the intrinsic ZPL width along with the acoustic–phonon pedestals in CdSe QDs. Contributions to the SHB response from the acoustic–phonon assisted transition show strong electron–phonon coupling in CdSe QDs, in agreement with theoretical expectation. The temperature dependence of the ZPL linewidth indicates that electron–phonon interactions contribute significantly to spectral broadening of the ZPL and suggest spin relaxation to dark states and thermal activation as likely mechanisms by which electron–phonon coupling induces decoherence for the ZPL. In spite of the stronger electron–phonon coupling, the decoherence rate for the ZPL in CdSe QDs is comparable to that in self-assembled InGaAs QDs. A comparison of the intrinsic ZPL linewidth in III–V and II-–VI based QDs, which feature significantly different electron–phonon coupling strengths, should provide the much needed information for developing a theoretical understanding on how electron–phonon interactions contribute to intrinsic decoherence in QDs.

This work has been supported in part by the NSF by Grant Nos. 0201784 (H. W.), 0303969, and 0305524 (D. S. C.), ARO, and DARPA-SPINS/ONR. The work of S.V.G. has been funded by US DOE.

[1] T. H. Stievater, X. Li, D. G. Steel, D. Gammon, D. S. Katzer, D. Park, C. Piermarocchi, and L. J. Sham, Phys. Rev. Lett. **87**, 133603 (2001); H. Kamada, H. Gotoh, J. Temmyo, T. Takagahara, and H. Ando, *ibid.* **87**, 246401 (2001); H. Htoon, T. Takagahara, D. Kulik, O. Baklenov, A. L. Holmes, Jr., and C. K. Shih, *ibid.* **88**, 087401 (2002).

[2] P. Michler, A. Kiraz, C. Becher, W. V. Schoenfeld, P. M. Petroff, L. Zhang, E. Hu, and A. Imamoglu, Science **290**, 2282 (2000); C. Santori, M. Pelton, G. Solomon, Y. Dale, and Y. Yamamoto, Phys. Rev. Lett. **86**, 1502 (2001).

[3] V. D. Kulakovskii, G. Bacher, R. Weigand, T. Kümmell, A. Forchel, E. Borovitskaya, K. Leonardi, and D. Hommel, Phys. Rev. Lett. **82**, 1780 (1999); T. Flissikowski, A. Hundt, M. Lowisch, M. Rabe, and F. Henneberger, *ibid.* **86**, 3172 (2001); L. Besombes, K. Kheng, L. Marsal, and H. Mariette, Phys. Rev. B **63**, 155307 (2001).

[4] J.-Y. Marzin, J.-M. Gérard, A. Izraël, D. Barrier, and G. Bastard, Phys. Rev. Lett. **73**, 716 (1994); M. Grundmann, J. Christen, N. N. Ledentsov, J. Böhrer, D. Bimberg, S. S. Ruvimov, P. Werner, U. Richter, U. Gösele, J. Heydenreich, V. M. Ustinov, A. Y. Egorov, A. E. Zhukov, P. S. Kopev, and Z. I. Alferov, *ibid.* **74**, 4043 (1995); M. Bayer and A. Forchel, Phys. Rev. B **65**, 041308 (2002).

[5] P. Borri, W. Langbein, S. Schneider, U. Woggon, R. L. Sellin, D. Ouyang, and D. Bimberg, Phys. Rev. Lett. **87**, 157401 (2001); D. Birkedal, K. Leosson, and J. M. Hvam, *ibid.* **87**, 227401 (2001).

[6] G. Mahan, *Many-Particle Physics* (Plenum, New York, 1990).

[7] S. Schmitt-Rink, D. A. B. Miller, and D. S. Chemla, Phys. Rev. B **35**, 8113 (1987).

[8] T. Takagahara, Phys. Rev. B **60**, 2638 (1999).

[9] B. Krummheuer, V. M. Axt, and T. Kuhn, Phys. Rev. B **65**, 195313 (2002).

[10] X. Fan, T. Takagahara, J. E. Cunningham, and H. Wang, Solid State Commun. **108**, 857 (1998).

[11] E. A. Muljarov and R. Zimmermann, arXiv: cond-mat/0312510 v1 (2003).

[12] S. V. Goupalov, R. A. Suris, P. Lavallard, and D. S. Citrin, IEEE J. Sel. Top. Quantum Electron. **8**, 1009 (2002); S. V. Goupalov and R. A. Suris (unpublished).

[13] S. Lee, I. Daruka, C. S. Kim, A.-L. Barabási, J. L. Merz, and J. K. Furdyna, Phys. Rev. Lett. **81**, 3479 (1998).

[14] P. Palinginis, S. Tavenner, M. Lonergan, and H. Wang, Phys. Rev. B **67**, 201307(R) (2003).

[15] J. Puls, M. Rabe, H.-J. Wünsche, and F. Henneberger, Phys. Rev. B **60**, R16303 (1999).

[16] A. Blacha, H. Presting, and M. Cardona, Phys. Status Solidi B **126**, 11 (1984).